









## Article

# Development of a Steam Generator Mock-Up for EU DEMO Fusion Reactor: Conceptual Design and Code Assessment

Alessandra Vannoni <sup>1</sup>, Pierdomenico Lorusso <sup>2,\*</sup>, Marica Eboli <sup>3</sup>, Fabio Giannetti <sup>1</sup>, Cristiano Ciurluini <sup>1</sup>,  
Amelia Tincani <sup>3</sup>, Ranieri Marinari <sup>3</sup>, Andrea Tarallo <sup>4</sup> and Alessandro Del Nevo <sup>3</sup>

<sup>1</sup> Department of Astronautical, Electrical and Energy Engineering (DIAEE), Sapienza University of Rome, 00186 Roma, Italy

<sup>2</sup> Department of Fusion and Nuclear Safety Technology (ENEA), 00044 Rome, Italy

<sup>3</sup> Department of Fusion and Nuclear Safety Technology (ENEA), Camugnano, 40032 Bologna, Italy

<sup>4</sup> CREATE Consortium, Università di Napoli Federico II, 80125 Napoli, Italy

\* Correspondence: pierdomenico.lorusso@enea.it; Tel.: +39-06-94005121

**Abstract:** Recent R&D activities in nuclear fusion have identified the DEMO reactor as the ITER successor, aiming at demonstrating the technical feasibility of fusion plants, along with their commercial exploitation. However, the pulsed operation of the machine causes an “unconventional” operation of the system, posing unique challenges to the functional feasibility of the steam generator, for which it is necessary to define and qualify a reference configuration for DEMO. In order to facilitate the transitions between different operational regimes, the Once Through Steam Generator (OTSG) is considered to be a suitable choice for the DEMO primary heat transfer systems, being characterized by lower thermal inertia with respect to the most common U-tube steam generators. In this framework, the ENEA has undertaken construction of the STEAM facility at Brasimone R.C., aiming at characterizing the behavior of the DEMO OTSG and related water coolant systems in steady-state and transient conditions. A dedicated OTSG mock-up has been conceived and designed, adopting a scaling procedure, keeping the height 1:1 of the DEMO OTSGs. The conceptual design has been supported by RELAP5/Mod3.3 thermal-hydraulic calculations. CFD and FEM codes have been used for fluid-dynamic analyses and mechanical stress analyses, respectively, in specific parts of the component.

**Keywords:** DEMO; water technologies; STEAM facility; experimental installation; once through steam generator (OTSG); RELAP5



**Citation:** Vannoni, A.; Lorusso, P.; Eboli, M.; Giannetti, F.; Ciurluini, C.; Tincani, A.; Marinari, R.; Tarallo, A.; Del Nevo, A. Development of a Steam Generator Mock-Up for EU DEMO Fusion Reactor: Conceptual Design and Code Assessment. *Energies* **2023**, *16*, 3729. <https://doi.org/10.3390/en16093729>

Academic Editor: Orlando Ayala

Received: 1 March 2023

Revised: 17 April 2023

Accepted: 24 April 2023

Published: 26 April 2023



**Copyright:** © 2023 by the authors. Licensee MDPI, Basel, Switzerland. This article is an open access article distributed under the terms and conditions of the Creative Commons Attribution (CC BY) license (<https://creativecommons.org/licenses/by/4.0/>).

## 1. Introduction

In recent years, relevant R&D activities on fusion technology have led to the conceptualization of the DEMO (DEMONstration Power Station) reactor [1], an evolution of the ITER experimental reactor [2]. These efforts aim at demonstrating the fusion reactor feasibility and its electricity production at competitive prices with respect to other energy sources [3]. The complexity of the fusion machine design has led European countries to focus their research efforts by founding EUROfusion, a European consortium for nuclear fusion development [4].

As a partner of the EUROfusion Consortium, ENEA (Italian National Agency for New Technologies, Energy and Sustainable Economic Development) pursues R&D activities to develop the Water Cooled Lithium Lead (WCLL) Breeding Blanket (BB) design [5], selected as the driver concept for DEMO, in the framework of the BB and Balance of Plant (BoP) work packages of the EUROfusion Power Plant Physics and Technology Programme.

One of the peculiar features of the fusion machines is the pulsed power generation from the plasma, which determines unique challenges to the functional feasibility of the components [6], especially of the heat sink (i.e., steam generator), making it necessary

to define reliable control logics, capable of distinguishing the operational transients (i.e., pulse-dwell-pulse phases) from the accidental ones.

The “unconventional” operation of the fusion reactor has led to the selection of the Once Through Steam Generator (OTSG) as the main heat sink [7] since it is characterized by lower thermal inertia with respect to the most common U-tube generators, and therefore, it is more suitable for following the variability of the power load. The research activity has to demonstrate the possibility of translating the well-proven Pressurizer Water Reactor (PWR) technology in a fusion reactor plant.

In this framework, a new multipurpose experimental infrastructure, named W-HYDRA, will be designed, constructed and operated at ENEA Brasimone R.C. Among the facilities constituting this new platform, STEAM [8] is designed to experimentally investigate the DEMO BoP, focusing on the Steam Generator (SG) of the BB Primary Heat Transfer Systems (PHTSs). The STEAM facility will be mainly made up of two loops reproducing the DEMO PHTS and Power Conversion System (PCS), respectively, thermally coupled by means of the test section (i.e., the OTSG), which is a scaled-down mock-up of the DEMO OTSGs.

A design activity has been performed to achieve a preliminary layout of the OTSG mock-up to be installed in the STEAM facility. Such a study has been supported by means of a Thermal-Hydraulic (TH) analysis of this component using the SYStem TH (SYS-TH) code RELAP5/Mod3.3 [9]. The conceptualization of the STEAM OTSG starts from the preliminary qualification of the RELAP5/Mod3.3 code against experimental data related to the correspondent component installed in the Three Mile Island (TMI) nuclear power plant. After that, the sizing of the Breeding Zone (BZ) OTSG has been performed and its TH performances during DEMO normal operations have been fully characterized [10]. Finally, a scaling procedure has been applied to the BZ OTSG to design the STEAM mock-up [8]. Different configurations have been analyzed with the RELAP5/Mod3.3 code and further optimization has been implemented to obtain a configuration suitable for the facility requirements. In addition, CFD analyses on the riser tube support plates (i.e., grids) and Thermo-Mechanical (TM) analyses on the tube sheet have been carried out and are presented in the following.

## 2. RELAP5/Mod3.3 Model Qualification through TMI OTSG Experimental Data

This paper focuses on the realization of a numerical model of the STEAM OTSG mock-up, aiming at supporting the design and the realization of the component and its integration in the circuit. The TH analysis and simulation of this component have been performed using the SYS-TH code RELAP5/Mod3.3.

A preliminary activity has been dedicated to the verification of the code capabilities in simulating the thermal-hydraulic behavior of an OTSG, in a configuration envisioned for the DEMO reactor. Among the builders of PWRs, Babcock and Wilcox (B&W) Company [11] is the only supplier of OTSGs [12,13]; therefore, the B&W OTSG of TMI power plant [14,15] has been taken as a reference for the analysis (see Figure 1, left). A 1-D numerical model has been set up using RELAP5/Mod3.3 (see Figure 2) reproducing both the primary side (PS), i.e., tube side, and the secondary side (SS), i.e., shell side, of the component.

RELAP5/Mod3.3 nodalization consists in an open loop that focuses on the component T/H investigation, neglecting the rest of the loop. Fluid boundary conditions (e.g., pressure and temperature) have been set by time-dependent volumes, while time-dependent junctions fix the mass flow rate.



into the annular downcomer (DC) between the shell and the shroud up to the water ports, where it changes its direction entering the riser (the shell side region between the primary tubes and the shroud). The tube bundle is structurally supported by 16 grids (tube support plates, TSPs) characterized by a mutual distance of approximately 1 m. The main feature of the OTSG is the recirculation zone, placed slightly above the feedwater inlet nozzles, which allows steam bleeding from the tube bundle in order to pre-heat the feedwater up to saturation conditions in correspondence with the tube bundle inlet. Flowing up through the tube bundle, the water vaporizes achieving superheated steam conditions on the top. Then, the steam is collected inside the annular DC and it exits toward the steam line.

The active length axial nodalization of both the primary and secondary sides respects the slice modeling approach. After mesh sensitivity, the selected mesh size for the thermal height is about 20 cm. Heat structures have been introduced in the model of Figure 2 to simulate the thermal coupling between the primary side and secondary side (i.e., the tube bundle with HS 310-1 and the lower and upper tube sheets with HS 113-3), allowing in such a way the power exchange along the OTSG active region. The model also includes heat structures reproducing the thermal losses toward the environment (HS 113-4 and 312-1). The axial meshing of the heat structures is the result of the slice modeling approach. The radial conduction has been taken into account by dividing the heat structure thickness (that contains also the insulation thickness for passive structures) into 14 intervals.

The model described above has been used to perform a set of simulations aiming at qualifying it for its utilization during the scaling process. Results showed that higher mass flows allow the exchange of higher power. For this reason, keeping the primary mass flow constant, feedwater mass flow is regulated by a control system in order to achieve the required outlet primary side temperature. A higher feedwater mass flow leads to a higher power exchange, resulting in a decrease in the primary side outlet temperature. On the other hand, the higher the feedwater mass flow rate, the lower the outlet steam temperature, affecting negatively the efficiency of the thermodynamic cycle. As reported in Table 1, the code results show good agreement with the reference data reported in [14], demonstrating that the model is suitable to support the design of this SG type and to investigate its TH performances.

**Table 1.** TMI steady state qualification.

Parameter	Unit	Ref [15]	R5	Error
Power	MW	1386	1335.27	3%
$T_{inlet,PS}$ (BC)	°C	318	318.00	0 °C
$T_{outlet,PS}$	°C	291	291.04	0.04 °C
$T_{inlet,SS}$ (BC)	°C	238	238	0 °C
$T_{outlet,SS}$	°C	299	305.11	6.11 °C
$P_{inlet,PS}$	MPa	15.17 [15]	15.02	−1%
$P_{outlet,PS}$	MPa	14.96	14.89	−0.5%
$P_{riser\ bottom,SS}$	MPa	N/A	6.52	-
$P_{outlet,SS}$	MPa	6.41	6.41	0%
$mfr_{PS}$ (BC)	kg/s	8801.1	8801.1	0%
$mfr_{SS}^*$	kg/s	761.59	717.80	−5.7%
$mfr_{rec}$	kg/s	N/A	111.1	-

\* Feedwater mass flow is regulated in order to exchange the amount of power that guarantees the correct primary side outlet temperature, which is considered to be fixed.

### 3. STEAM OTSG Mock-Up

The STEAM facility's [8] main purpose is to demonstrate the DEMO OTSG [16] feasibility and its capability to exchange the produced power in all phases foreseen during DEMO normal operations (i.e., pulse, dwell and related transitions). For this reason, once the RELAP5 model has been qualified, an analytical methodology is developed to perform a preliminary evaluation and sizing of the DEMO WCLL BB PHTS OTSGs, leading to the



thermal length reduction from 17 to 13 m. In doing so, the TSPs number has been reduced to 13, keeping the mutual distance of 1 m.

A scaling procedure has been then followed by applying the “power to volume” approach and keeping the full-length scale of the BZ OTSG. Assuming that the “power/tube” ratio is unchanged, and knowing the thermal loads, a mock-up (scaled 1:1 in length) has been conceived for the STEAM facility (3 MW).

Results of the scaling process show no major TH distortion nor instabilities but, keeping the same layout of the reference case, the obtained configuration has a DC annular gap 2 cm thick, which cannot be easily realized because of manufacturing tolerances of the coaxial pipes. Moreover, such a configuration would imply unavoidable distortions in preserving the pressure drop chain of the component, as well as issues with the installation of the instrumentation in the riser. For this reason, two different constructive solutions have been investigated, with one or two external DC tubes, respectively (Figure 3). This variation is pursued by adopting the DC scaled area for the case with one external pipe, and its half value for both the DCs in the case with two external pipes.

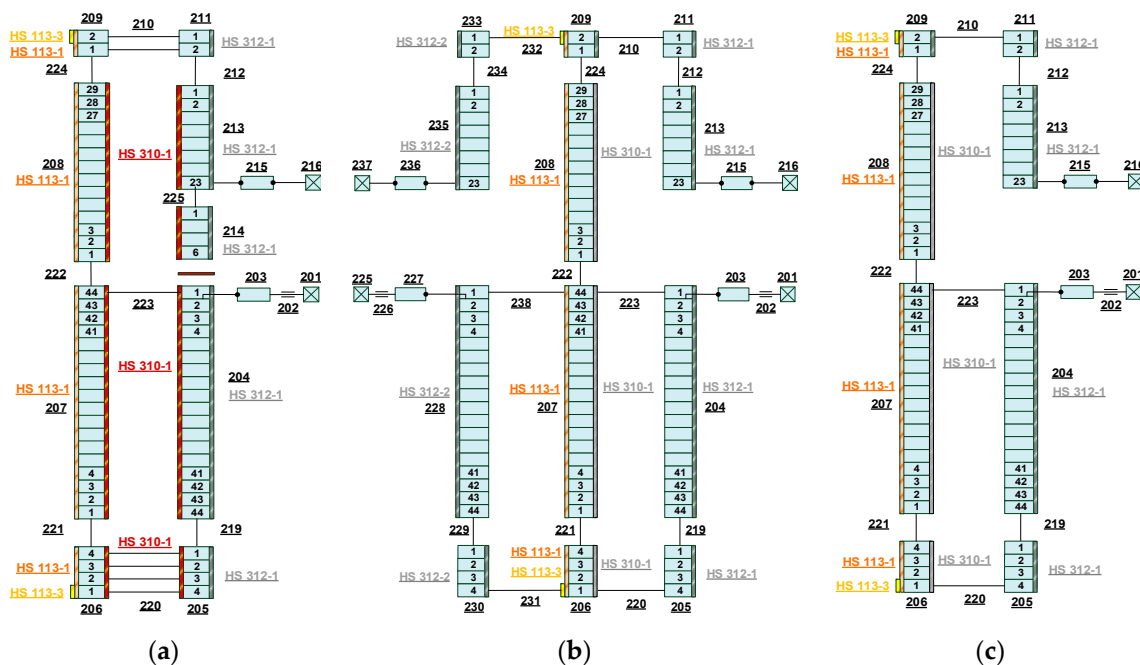


**Figure 3.** Analyzed configuration for the STEAM OTSG secondary side: annular coaxial DC (a), one external DC pipe (b), two external DC pipes (c).

The adoption of one (or two) DC pipe(s) leads to the following distortions, which refer to Figure 3:

- DC hydraulic diameter variation introduces distortions in the pressure drops;
- the steam DC dead zone (below pipes 213 and 235) is neglected, without determining any influence on the results;
- the dimensions of the inlet and outlet nozzles have not been scaled from TMI, but they have been assumed as the ones corresponding to the STEAM pipelines, introducing distortions of the correspondent pressure drops;
- the Aspirator Port (AP), is simulated by the Single Junction (SJ) 223 both in the integrated DC and one external pipe DC configurations, while in the two external DCs case, the total recirculation area is split in half with SJ 223 and SJ 238. This causes differences in the pressure loss coefficients calculated across the riser-AP and AP-DC;
- the multiple junction 220 used in the reference model of Figure 3a, simulating the eight Water Ports (WPs) that allow the feedwater to enter the tube bundle has been substituted with one (or two) SJ(s), for the case with one (or two) external DC(s).

Such differences cause distortions of the singular pressure drops among the three configurations;

- the shroud thickness has been changed accordingly to the different pressure it has to withstand in the case of integrated DC and one (or two) external DCs.

Table 2 summarizes the results of the simulations performed. As the main outcome, it is possible to conclude that, from a thermal-hydraulic point of view, the three OTSG configurations have almost the same performances as the BZ reference case, meaning that the scaling procedure has preserved the main features of the component.

**Table 2.** Comparison of the T/H results of the different configurations simulated.

Parameter	BZ	STEAM		
		Annular DC	One DC	Two DCs
Power [MW]	581.5	3.01	3.02	3.01
Riser Level [m]	1.8	1.75	1.86	1.86
DC Level [m]	4.0	3.94	3.50	3.49
$T_{\text{out,PHTS}}$ [°C]	295.0	294.87	294.78	294.75
$\Gamma_{\text{PHTS}}$ [kg/s]	3010.6	15.552	15.552	15.552
$\Gamma_{\text{FW}}$ [kg/s]	316.2	1.567	1.567	1.567
$\Gamma_{\text{rec}}$ [kg/s]	42.0	0.24	0.22	0.22
$\Gamma_{\text{rec}}/\Gamma_{\text{FW}}$	14	15	14	14
Heat losses	14.0	0.23	2.17	2.96
$P_{\text{loss}}/P$	0.02%	0.08%	0.72%	0.98%
Void F. (DC last volume)	0.34	0.02728	$4.0 \times 10^{-6}$	$1.0 \times 10^{-5}$

The thermal decoupling of the riser and downcomer affects the heat losses toward the environment. In particular, Table 2 shows that the percentage of the heat losses increases with decreasing the power (i.e., the vessel O.D.) and with realizing external DC(s), since the ratio surface/volume of the component increases. The higher value of heat losses (0.98%) is achieved in the case of two external DCs. Heat losses also affect the values of void fraction achieved at the bottom of the DC, obtained by injecting a recirculation flow through the AP for the pre-heating along the DC. Since the heat losses along the DC increase, the final value of the void fraction at the DC bottom decreases, passing from the integrated DC solution to cases with external DC(s). However, the results show that the recirculation flow rate is still sufficient for bringing the fluid to saturation before entering the tube bundle.

Pressure drop is the parameter that is mostly affected by the DC configuration variations. The superficial roughness adopted for the distributed pressure drop is  $4 \times 10^{-5}$  m. The adoption of one (or two) DC(s) led to the necessity of collapsing the annular DC and its related junction areas into one (or two). As a result, pressure loss coefficients and hydraulic diameters have been modified (see Table 3 and Figure 4).

**Table 3.** Comparison between pressure drops of the analyzed configurations.

Pressure Drops [kPa]	BZ	STEAM		
		Annular DC	One DC	Two DCs
PHTS * (from A to B)	81.94	118.26	118.21	118.23
DC (from 1 to 2)	−31.85	−31.69	−30.97	−30.17
Orifice plate (from 2 to 3)	2.26	2.62	2.15	2.16
WPs and low riser (from 3 to 4)	28.09	28.45	28.32	27.69
High riser (from 4 to 5)	4.04	16.74	16.66	17.18
Steam ports (from 5 to 6)	16.19	1.01	3.32	3.36
Steam DC (from 6 to 7)	0.61	9.77	0.62	1.62
Steam nozzle (from 7 to 8)	23.89	1.79	1.68	1.83
Total SS (from 1 to 8)	43.22	28.69	21.78	23.67
Aspirator port (from 4 to 9)	1.40	0.62	0.51	0.31

\* Primary side total pressure drops are calculated by subtracting the static contribution to the total pressure drop.

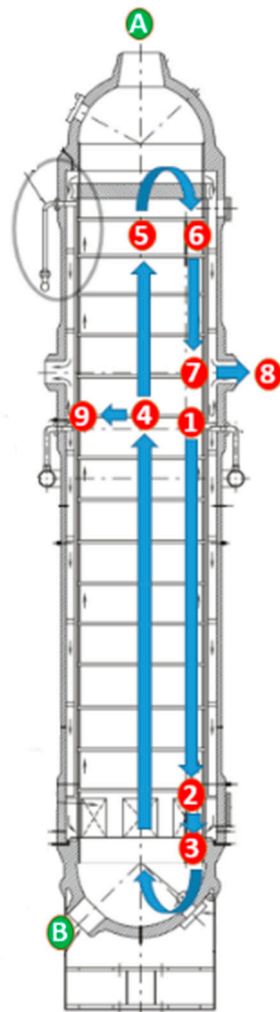


**Figure 4.** Pressure drops relevant points reported in Table 3 along the OTSG.

Stating that it is possible to conclude that the configuration with one external DCs (Figure 5) is a suitable choice for the OTSG mock-up foreseen for STEAM. In fact, assuring the removal of the required power, with respect to the full-size reference OTSG configuration, it:

- introduces low-pressure drop distortions;
- avoids parallel channels instability (which can occur in the two external-downcomer configurations);
- eliminates the problem related to the manufacturing of an integrated annular DC.

Table 4 summarizes the OTSG geometrical data of TMI, BZ, scaled and optimized STEAM. After the selection of the reference DC configuration, further optimizations have been implemented without introducing modifications to the primary side tube geometry (i.e., tube thickness, diameter, arrangement and pitch). In particular:

- according to the scaling procedure, the primary side tubes should be 35. Since the corresponding bundle configuration would be made up of uncompleted ranks, 37 tubes have been adopted in order to reduce the side effect: primary side flow area is increased and the fluid velocity is consequently decreased, affecting the heat transfer coefficient. However, the negative effect of the flow area increment is negligible with respect to the positive effect linked to the heat exchange area increment;
- in order to reduce the by-pass and to uniform the temperature of the fluid exiting from different sub-channels, the shell has been hexagonally shaped, preserving the scaled riser free flow area, as shown in Figure 6.

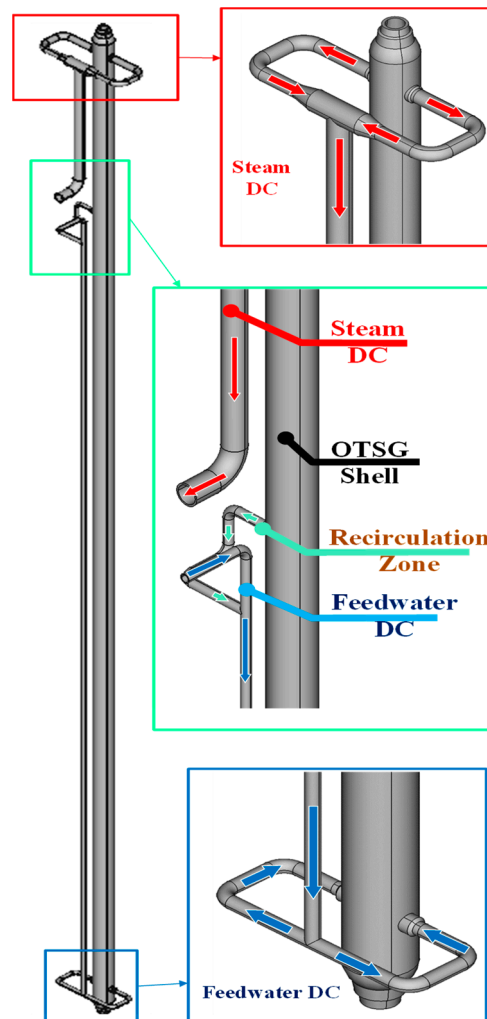


Figure 5. STEAM OTSG 3D CAD.

Table 4. TMI, BZ, STEAM scaled and optimized configuration geometrical data.

Parameter	TMI	BZ	STEAM (Scaled)	STEAM (Optim.)
Tubes number [-]	15,500	6943	35	37
Active Length [m]	16.269	12.98	12.98	12.98
Tubes O.D. [mm]	15.875	15.875	15.875	15.875
Total PHTS Area [m <sup>2</sup> ]	2.4367	1.09	0.0055	0.0058
Riser flow Area [m <sup>2</sup> ]	4.016	1.79	0.009	0.009
DC flow Area [m <sup>2</sup> ]	2.167	0.97	0.0049	0.0049
Rec. Area [m <sup>2</sup> ]	0.96	0.51	0.0026	0.0026
(p/D)	1.4	1.4	1.4	1.4
Lattice	Triangular	Triangular	Triangular	Triangular
Shell I.D. [m]	3.5	2.364	0.17	0.1554 (hexagon diameter)

In Figure 7 the temperature axial profile of BZ [10] and STEAM OTSG are shown: the feedwater temperature inside the downcomer steeply rises thanks to the recirculation pre-heating, reaching saturation conditions. Saturated boiling starts in the fluid flowing upwards in the riser until a single phase (superheating zone) is reached: the fluid temperature starts to increase, remaining constant inside the steam downcomer, where the heat transfer coefficient is almost negligible. The primary side temperature profile is flatter

in the upper part of the OTSG because of the small heat transfer coefficient of the steam secondary side, while the lower part of the profile is steeper due to the high saturated boiling heat transfer coefficient.

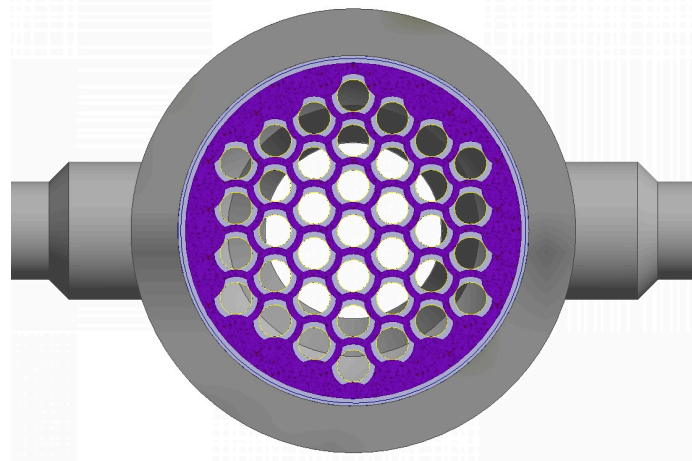


Figure 6. Hexagonally shaped riser with a detail of the tube support plate (TSP).

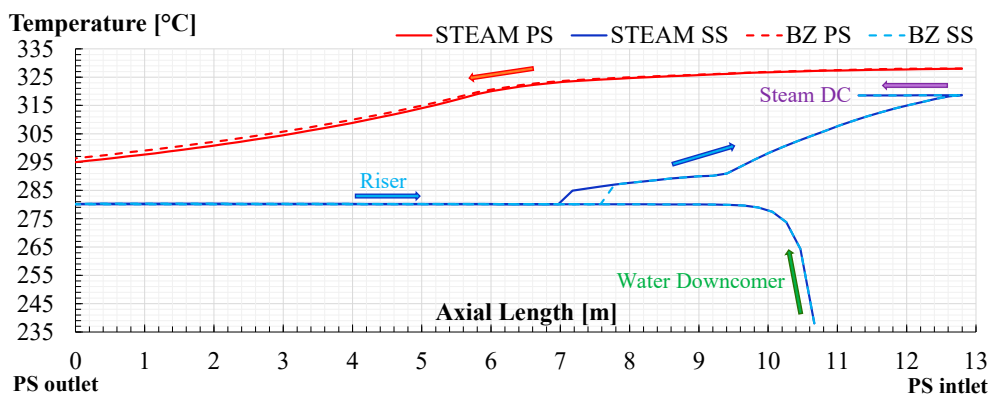


Figure 7. Axial temperature profile of BZ and STEAM OTSG.

The secondary side heat transfer coefficient in the riser is shown in Figure 8. Starting from the riser inlet, the nucleated boiling region is characterized by turbulences resulting from the bubble formation that enhances the heat transfer coefficient, until dry-out occurs when a blanket of saturated steam forms on the tube’s internal surface. Film boiling, characterized by a low heat transfer coefficient, starts and lasts until 100% steam quality is reached. After the end of the two-phase region, the superheating region starts, where the heat transfer coefficient is lower due to the low vapor density.

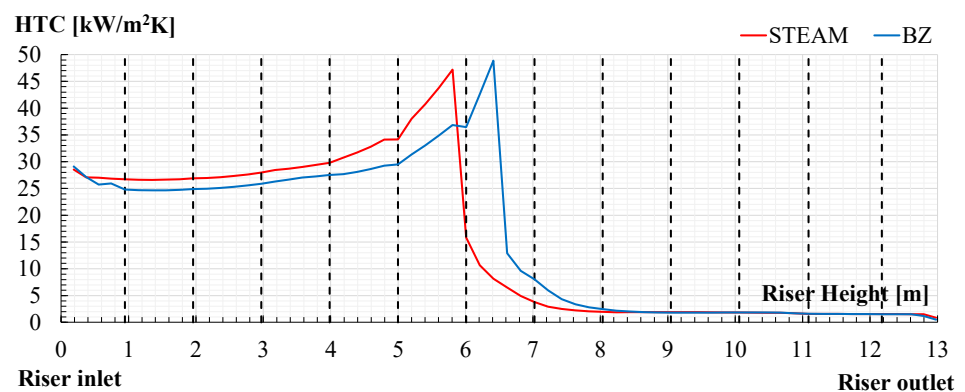


Figure 8. Axial profile of the heat transfer coefficient of BZ and STEAM OTSG.



In Figures 7 and 8, the main effect of the optimization process can be detected: as a result of the primary side tube number increase, dry-out occurs at a lower height in STEAM with respect to BZ OTSG, and therefore, also the vapor temperature starts to increase at a lower height.

#### 4. CFD Analyses on the OTSG Tube Support Plate

System thermal hydraulic codes such as RELAP code are not reliable in the prediction of local pressure losses such as flow distribution in manifolds or sudden flow area changes. To overcome this issue a CFD analysis with Ansys CFX 2022 [17] code has been performed in order to hydraulically characterize the Tube Supporting Plate (TSP), reported in Figure 9, to assess the concentrated pressure drops at different mass flow rates (Re number). The ratio between TSP broached area and the riser free flow area is 0.01.

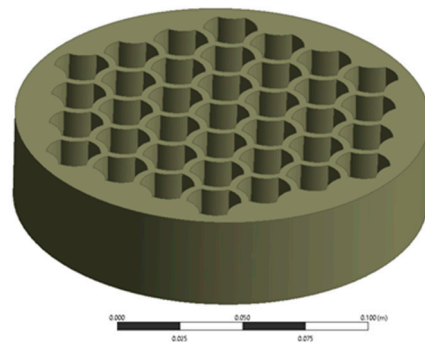


Figure 9. Three-dimensional model of the tube supporting plate.

The developed CFD model includes only the fluid part and it is based on the same geometrical dimensions of the RELAP5 input, preserving the hexagon dimension, the grid measures, the PS tube diameter and the pitch. The 3D geometry, reported in Figure 10, consists of:

- an upstream zone: a tube bundle region whose length is equal to 57 hydraulic diameters in order to have fully developed flow conditions at the grid;
- the tube support plate;
- a downstream zone: a tube bundle region whose length is equal to 25 hydraulic diameters in order to take into account the flow recirculation downstream the grid in the simulations.

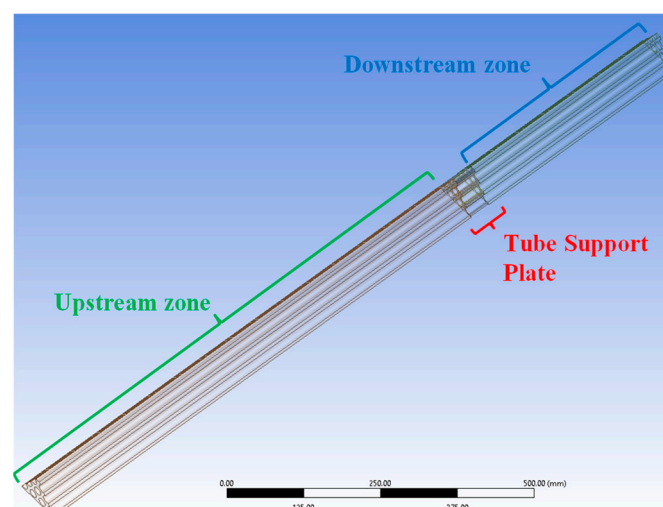
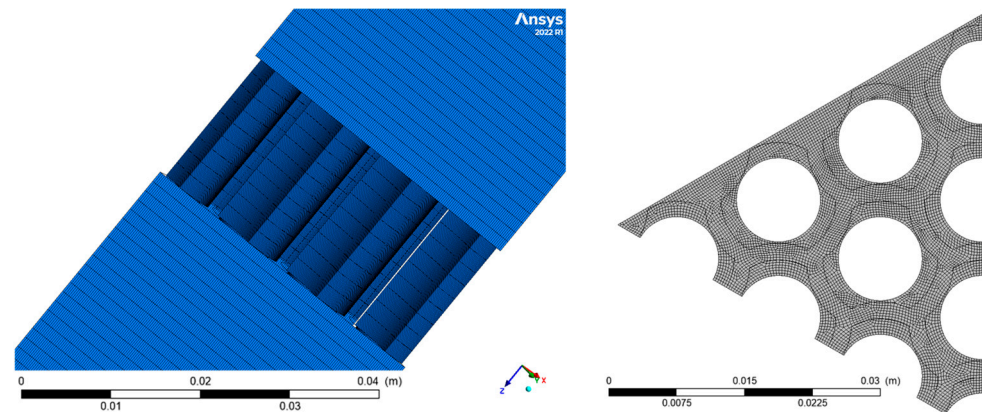


Figure 10. Sketch of the 3d geometry developed highlighting the three main regions of the model.

Thanks to the symmetry of the pipe triangular lattice, only 1/6 of the geometry has been modeled, this solution grants a reduction of the computational resources for the simulations.

The input mesh (Figure 11) is fully structured both in the upstream/downstream regions and in the TSP grid (Figure 6). The average mesh size is 0.3 mm in the upstream/downstream regions and 0.2 mm inside the TSP holes. No node inflation was set on the walls, the water viscous sublayer is resolved with wall functions. The total number of elements is 9.97 million while the total number of nodes is 10.32 million.



**Figure 11.** Axial sketch of the fully structured mesh developed (left) and highlight of the calculation grid on a cross-section plane (right).

Several calculations have been performed in order to characterize the grid pressure drops and the relative loss coefficient at different flow conditions. Isothermal simulations with single-phase fluid in saturation conditions (liquid or vapor) have been set adopting variable mass flow (from 1% to 100% of the nominal value) corresponding to a Reynolds number ranging from 300 to  $1.5 \times 10^5$ . Single-phase fluid simulations were performed instead of the two-phase ones, due to the well-known limitation of the current CFD codes in the reliable (validated) prediction of two-phase flow regimes. To overcome this issue, the Re range of the CFD simulation was widely expanded if compared to the nominal operating conditions in order to support the RELAP5 code, bordering all the possible Re flow regimes of the liquid and vapor phases in the OTSG. A detailed overview of the test conditions is reported in Table 5.

**Table 5.** CFD numerical test matrix.

Phase	$\dot{m}$	Re	Regime	$mfr_{CFD}$	$v$
[-]	[%]	[-]	[-]	[kg/s]	[m/s]
liq	100	$3.0 \times 10^4$	Turb	0.272	0.24
liq	50	$1.5 \times 10^4$	Tran	0.136	0.119
liq	25	$7.5 \times 10^3$	Tran	0.068	0.059
liq	10	$3.0 \times 10^3$	Tran	0.027	0.023
liq	6	$1.8 \times 10^3$	Tran	0.016	0.014
liq	4	$1.2 \times 10^3$	Lam	0.011	0.009
liq	3	$9.0 \times 10^2$	Lam	0.008	0.007
liq	1	$3.0 \times 10^2$	Lam	0.003	0.002
vap	100	$1.5 \times 10^5$	Turb	0.272	5.41
vap	50	$7.5 \times 10^4$	Turb	0.136	2.704
vap	25	$3.7 \times 10^4$	Turb	0.068	1.352
vap	17	$2.5 \times 10^4$	Turb	0.045	0.9
vap	1	$1.5 \times 10^3$	Lam	0.003	0.054

The boundary conditions set in the input model are:

- a mass flow rate at the inlet surface (1/6 of the nominal value), see  $mfr_{CFD}$  in Table 5;
- an average relative pressure of 0 Pa at the outlet surface;
- a free slip boundary condition (zero friction) on the side walls due to the symmetry constraint of the model.

Water and steam properties at saturated conditions (6.41 MPa, 279.93 °C) were calculated from [18] and implemented in the CFX code.

The turbulence model set in the simulations is the SST  $k-\omega$  developed by Menter [19] for the turbulent and transition flow regime while a laminar flow model is set for the laminar regime. The simulations performed are steady-state RANS followed by a small transient run ( $CFL \approx 1$ ) of 3 s total time to reduce and stabilize all the RMS residuals to a value of  $10 \times 10^{-5}$ . Total pressure drops across the model and velocity components on two monitor points upstream and downstream of the TSP were also monitored during the simulations.

Thanks to the Upgraded Cheng and Todreas (UCT) pressure drop correlation [20] for bare rod bundles, laminar and turbulent Re number limits were calculated. The maximum Re number for the laminar region is 1532 while the minimum Re for the turbulent regime is 19,055. It must be highlighted that the transition flow range predicted by the correlation is wider than the one implemented in RELAP5/Mod3.3 [9]. Four cases are in the laminar flow regime, four cases are in the transition regime and five cases are in the fully turbulent regime.

The axial pressure profile of a general test case (Figure 12) shows: a linear gradient from the inlet to the TSP due to the distributed pressure drop in the tube bundle, a step pressure drop and downstream pressure recovery due to the localized pressure drop of the TSP followed by the liner pressure trend of the downstream tube bundle.

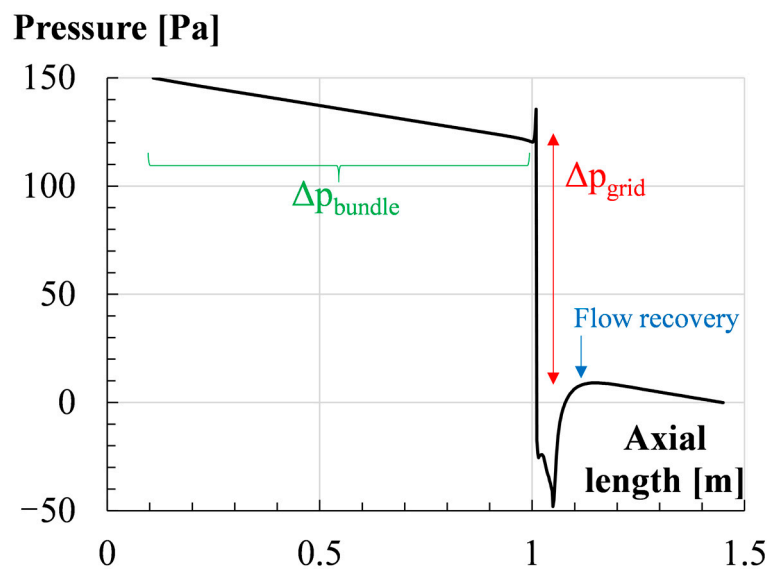


**Figure 12.** Axial pressure profile for a generic test case (100% liquid mass flow rate).

To assess the reliability of the model and mesh developed, the pressure gradients in the tube bundle were compared with the analytical correlation [20] for all the cases simulated. The accuracy of the Upgraded Cheng and Todreas (UCT) pressure drop correlation for bare rod bundles is about  $\pm 10\%$  for all the flow regimes [21], as reported in Table 6 the discrepancy of the CFD results is always lower than 7% for all the cases confirming the reliability of the CFD results.

**Table 6.** Relative error of the bundle pressure gradient predicted by the CFD simulations against the analytical UCT correlation.

Re	Regime	$(\frac{dp}{dl})_{UCT}$	$(\frac{dp}{dl})_{CFD}$	Err = $\frac{ UCT-CFD }{UCT}$
[-]	[-]	[Pa/m]	[Pa/m]	[-]
$3.0 \times 10^4$	Laminar	30.56	31.88	0.04
$1.5 \times 10^4$	Laminar	8.83	9.52	0.07
$7.5 \times 10^3$	Laminar	2.79	2.93	0.05
$3.0 \times 10^3$	Laminar	0.66	0.67	0.01
$1.8 \times 10^3$	Transition	0.31	0.30	0.02
$1.2 \times 10^3$	Transition	0.16	0.17	0.05
$9.0 \times 10^2$	Transition	0.12	0.12	0.02
$3.0 \times 10^2$	Transition	0.04	0.04	0.05
$1.5 \times 10^5$	Turbulent	518.05	499.82	0.04
$7.5 \times 10^4$	Turbulent	146.72	144.93	0.01
$3.7 \times 10^4$	Turbulent	41.56	42.65	0.03
$2.5 \times 10^4$	Turbulent	19.83	20.97	0.05
$1.5 \times 10^3$	Turbulent	0.18	0.19	0.07

Figure 13 shows in semi-logarithmic scale the TSP local pressure loss coefficient ( $K_{grid}$ ) against the Re number. The parameter  $K_{grid}$  is defined as:

$$K_{grid} = \frac{\Delta p_{grid}}{\frac{1}{2}\rho v^2}, \tag{1}$$

where  $\Delta p_{grid}$  is the concentrated pressure loss due to the TSP grid and highlighted in Figure 12,  $\rho$  is the fluid density while  $v$  is the average mainstream velocity of the fluid in the tube bundle upstream of the TSP.

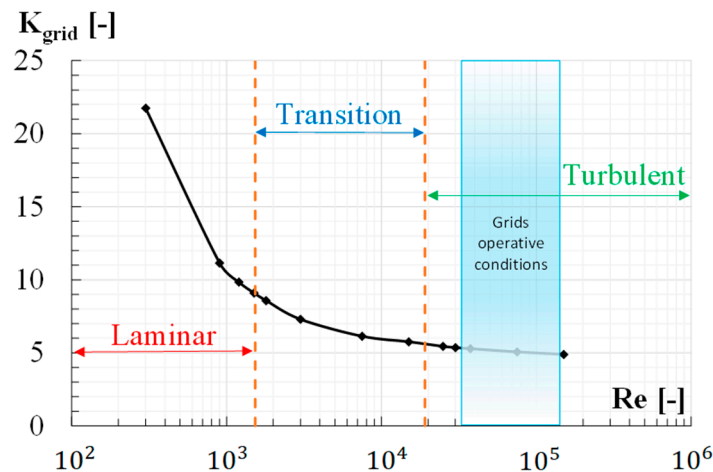


**Figure 13.** Plot of the TSP local pressure drop coefficient against the bundle Re number, In the plot are highlighted the flow regimes and the Re operative range near the grids according to RELAP results.

The general trend is similar to the Darcy friction factor coefficient with an almost linear trend in the laminar region and a power law trend in the transition/turbulent region. In the same figure is also reported (in light blue) the range of the average Re near the TSPs coming from the steady-state RELAP5 simulations.

### 5. Thermo-Mechanical Design of the STEAM OTSG Tubesheet

The STEAM OTSG is a non-nuclear equipment and falls into the PED hazard Category IV. The PED does not prescribe a specific standard for design; therefore, the analyses

have been performed referring to the well-known ASME Boiler and Pressure Vessel Code (B&PVC). The pressure vessel (i.e., the shell) is assumed to be constructed from an 8-inch Schedule 160 carbon steel pipe and the tubesheet is considered to be integrated with the shell and channels (Figure 14). Future design activities will explore a more convenient flanged design. Concerning the internals of the STEAM OTSG mock-up, the TSPs are  $1\frac{1}{2}$  inches in thickness, as in TMI OTSG. A 1/8-inch-thick hexagonal shroud is placed around the tube bundle, forming the secondary-side flow channel.

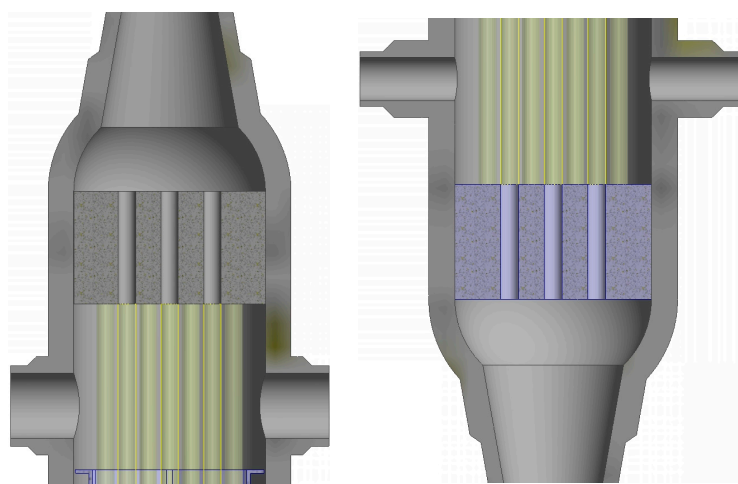


**Figure 14.** Upper (left) and lower (right) tubesheets.

ASME SA106 grade B carbon steel is commonly used in the construction of high-temperature oil and gas equipment, boilers, etc., and thus was assumed as the main structural material, due to its good resistance to high temperatures, low price, and good weldability. The thickness selected in any case far exceeds what would be required to withstand pressure load, but it was increased to consider possible unreinforced penetrations for measurement equipment, ports, centering pins, etc. The tube material is Inconel<sup>®</sup> Alloy 690 (UNS N06690). The allowable stress calculation procedure provided by the PED may lead to limits different from those taken from ASME B&PVC Section II-D. However, possible changes in material choice will be addressed in more detailed stages of the design. The tubesheet was preliminarily dimensioned according to the iterative methodology suggested by ASME BPVC.VIII.1 Part. UHX-13. Therefore, seven loading cases were considered: three design conditions that do not include thermal stresses and four operating conditions that do also include the thermal stresses. The load cases are summarized in Table 7.

**Table 7.** Loading cases for tubesheet preliminary sizing.

Case	$P_s$ MPa	$P_t$ MPa	$T_s$ °C	$T_t$ °C
1	0	17.8	N.C.	N.C.
2	7.4	0	N.C.	N.C.
3	7.4	17.8	N.C.	N.C.
4	0	15.5	287	311
5	6.4	0	287	311
6	6.4	15.5	287	311
7	0	0	287	311

The tubes were assumed to be fully hydraulically expanded into the tubesheet holes and then welded primary side. Corroded conditions were not considered.

Eventually, the thickness of the tubesheet was set to 4. The results are shown in Tables 8 and 9.



**Table 8.** Results for design loading cases.

	Limit	Unit	Case 1	Case 2	Case 3
Tubesheet Bending stress	141.8	MPa	12.3	9.1	12.0
Tube compressive load	63.5	MPa	35.8	14.6	21.2
Shell membrane stress	94.5	MPa	2.8	10.1	12.7
Total shell axial stress	141.8	MPa	5.4	41.0	40.6
Total channel axial stress	141.8	MPa	70.2	6.6	76.3

**Table 9.** Results for operating loading cases.

	Limit	Unit	Case 4	Case 5	Case 6	Case 7
Tubesheet Bending stress	283.5	MPa	6.5	13.1	3.2	13.7
Tube compressive load	63.4	MPa	87.3	131.3	100.1	118.4
Shell membrane stress	283.5	MPa	16.9	23.4	25.7	14.5
Total shell axial stress	283.5	MPa	24.9	60.9	60.6	24.7
Total channel axial stress	283.5	MPa	50.9	4.7	56.3	10.2

As one can see, the stresses are everywhere far lower than the allowable limits, except in operating conditions when the compression stress in the tubes due to the thermal gradient would be more than allowed. This is a well-known issue that affects this kind of steam generator; therefore, to withstand the thermal loads, the tubes shall be pretensioned before mounting (e.g., once welded to the one tubesheet, they may be heated up and then welded to the other tubesheet). A preliminary Finite Element Method (FEM) steady-state thermo-mechanical analysis was conducted with ANSYS® Mechanical 2021 R2 to validate ASME design-by-formulae results. A 90° sector of the upper head was modeled (Figure 15).

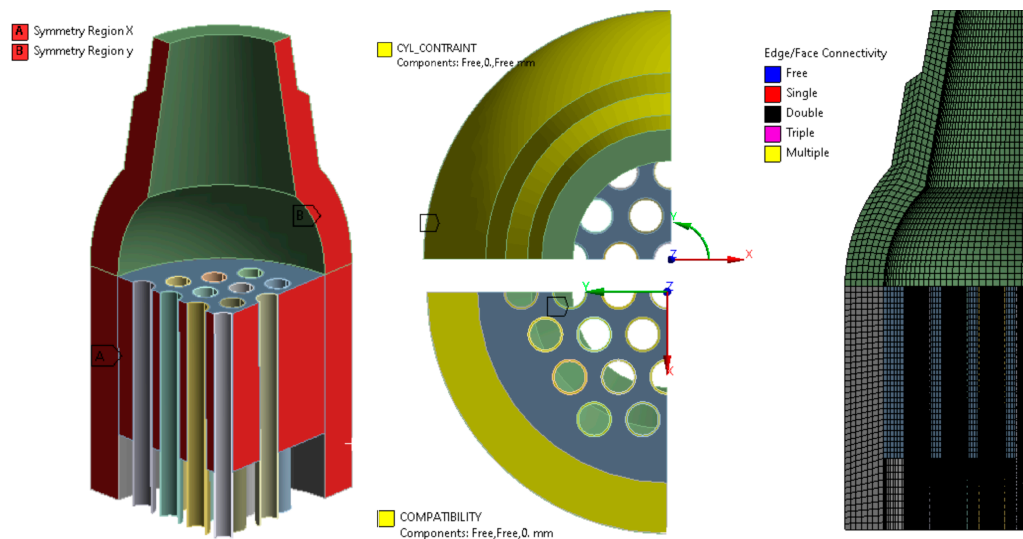


**Figure 15.** Solid model for FE thermal analyses.

The OTSG was considered perfectly insulated. Equilibrium temperatures were assigned to fluid and steam domains. The results (Figure 16) were then imported into ANSYS Mechanical.

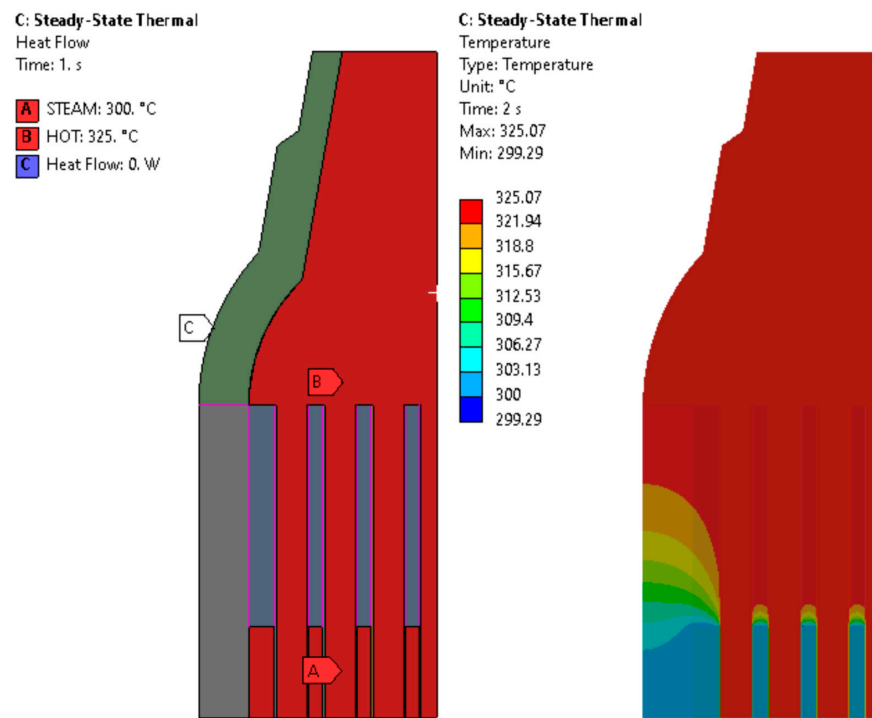


Figure 16. Thermomechanical analysis.

For the sake of conciseness, just some results related to the normal operating conditions are summarised in Figure 17 and Table 10.

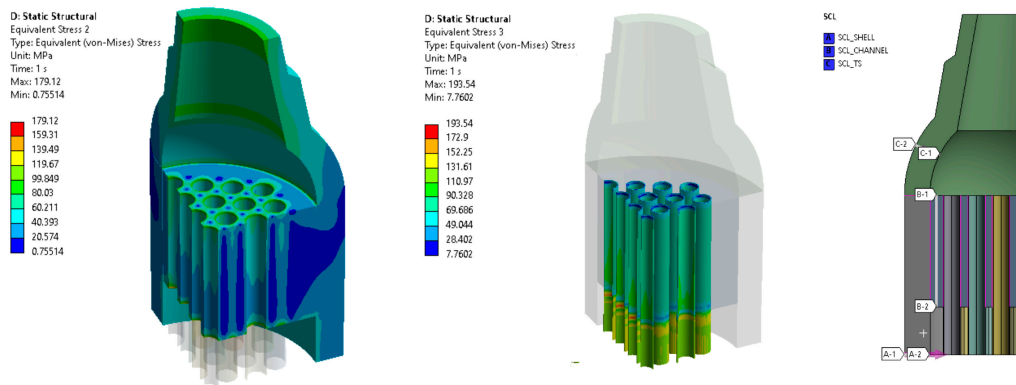


Figure 17. Von-Mises stresses and SCLs are used for stress linearization (normal operation loading case).

Table 10. FEA results for normal operation loading cases.

	LIMIT	Unit	ASME	FEA
Max Tubesheet Bending stress	283.5	MPa	3.2	6.01
Tube compressive load	63.4	MPa	100.1	95.8
Shell membrane stress	283.5	MPa	25.7	29.4
Total shell axial stress	283.5	MPa	60.6	47.6
Total channel axial stress	283.5	MPa	56.3	63.0

The results obtained from FEA are close to ASME previsions, although, as mentioned, the design of the OTSG shall be optimized in more detailed phases of the design.

## 6. Conclusions

The present paper describes the outcomes of the preliminary design phase of the DEMO OTSG mock-up to be installed in the STEAM facility, which will be built at the ENEA Brasimone Research Centre. The infrastructure is conceived to validate the WCLL DEMO BoP water coolant systems through a series of steady-state and transient experiments, aiming at demonstrating the capability of the OTSG to follow the plasma-induced load variations.

The first part of the activity focused on the realization of a RELAP5/Mod3.3 model to be used for code validation through the reproduction of the TMI OTSG. An analytical methodology has been set up in order to perform the BZ OTSG sizing, defining the active length on the basis of the power requirement. The procedure leads to a reduction in the tube length from 17 m of the TMI OTSG to 13 m. The obtained geometry can be considered the reference configuration to which apply a 1:1 in length scaling procedure for the STEAM OTSG through the adoption of a scaling factor calculated as powers ratio.

The constant “power to volume” scaling to switch from BZ OTSG to STEAM OTSG does not affect the parameter stability nor introduce major TH distortions. However, keeping the same layout of the BZ OTSG, the obtained configuration is characterized by a downcomer gap thickness of 2 cm, which is unfeasible because of manufacturing tolerances of coaxial pipes and determines remarkable difficulties in the instrumentation installation in the annular region. Two different solutions have been investigated with one or two external downcomers without modifying the component total flow area but removing the thermal coupling between ascendant and descendant regions. RELAP5/Mod3.3 comparison of the different constructive options shows that heat losses to the environment in percentage increases in decreasing power and in realizing external DC(s). Pressure losses are also influenced by the configuration variation since the necessity of collapsing the annular DC area and its related junctions into one (or two) modifies the correspondent pressure loss coefficients and hydraulic diameter. The solution with one external downcomer has been selected as a reference layout for the OTSG mock-up to be tested in the dedicated facility STEAM since it is easier to realize and does not introduce relevant distortions nor determine flow instabilities.

Further improvements have been adopted for optimizing the obtained configuration, such as increasing the scaled number of PS tubes in order to complete the ranks and adopting a hexagonally shaped riser in order to reduce the side effect. As a result, the final mock-up is characterized by a higher exchange area with respect to the required one determining anticipation of the dry-out condition.

CFD analyses have been performed in order to hydraulically characterize the TSP in order to find a Reynolds-dependent curve of the correspondent loss coefficient, to be implemented in RELAP5 code. Finally, FEM analyses have been carried out in order to size the tubesheets of the mock-up.

**Author Contributions:** Conceptualization, A.V., P.L., A.D.N. and M.E.; methodology, A.V., P.L. and A.D.N.; software, A.V., F.G., C.C., R.M. and A.T. (Andrea Tarallo); validation, A.V., P.L. and A.D.N.; formal analysis, A.V., P.L. and A.D.N.; investigation, A.V., P.L., A.D.N., M.E., F.G., R.M. and C.C.; resources, A.D.N.; data curation, A.V. and P.L.; writing—original draft preparation, A.V., P.L. and R.M.; writing—review and editing, A.V., P.L., M.E., F.G., C.C., A.T. (Amelia Tincani) and A.D.N.; visualization, A.V. and P.L.; supervision, A.D.N., M.E. and F.G.; project administration, A.D.N. and M.E.; funding acquisition, A.D.N. All authors have read and agreed to the published version of the manuscript.

**Funding:** This research was funded by the European Union via the Euratom Research and Training Programme, grant number 101052200.

**Institutional Review Board Statement:** Not applicable.

**Informed Consent Statement:** Not applicable.

**Data Availability Statement:** Not Applicable.

**Acknowledgments:** This work has been carried out within the framework of the EUROfusion Consortium, funded by the European Union via the Euratom Research and Training Programme (Grant Agreement No 101052200—EUROfusion). Views and opinions expressed are, however, those of the author(s) only and do not necessarily reflect those of the European Union or the European Commission. Neither the European Union nor the European Commission can be held responsible for them.

**Conflicts of Interest:** The authors declare no conflict of interest. The funders had no role in the design of the study; in the collection, analyses, or interpretation of data; in the writing of the manuscript; or in the decision to publish the results.

## Nomenclature

AP	Aspirator Port
BB	Breeding Blanket
BoP	Balance of Plant
BZ	Breeding Zone
B&W	Babcock & Wilcox
CFD	Computational Fluid Dynamics
DC	DownComer
DEMO	DEMONstration Power Plant
ENEA	Italian National Agency for New Technologies, Energy and Sustainable Economic Development
FEM	Finite Element Method
HS	Heat Structure
HYDRA	HYDRAulic
ITER	International Thermonuclear Experimental Reactor
MFR	Mass Flow Rate
N.C.	Not Considered
O.D.	Outer Diameter
OTSG	Once Trough Steam Generator
PCS	Power Conversion System
PHTS	Primary Heat Transfer System
PS	Primary Side
PWR	Pressurized Water Reactor
R&D	Research & Development
SG	Steam Generator
SJ	Single Junction
SS	Secondary Side
T-H	Thermal-Hydraulic
T-M	Thermo-Mechanical
TMI	Three Miles Island
TSP	Tuве Support Plate
UCT	Upgraded Cheng and Todreas
WCLL	Water Cooled Lithium Lead
WP	Water Port

## References

1. Federici, G.; Boccaccini, L.; Cismondi, F.; Gasparotto, M.; Poitevin, Y.; Ricapito, I. An overview of the EU breeding blanket design strategy as an integral part of the DEMO design effort. *Fusion Eng. Des.* **2019**, *141*, 30–42. [CrossRef]
2. Muratov, V.P.; Saksagansky, G.L.; Filatov, O.G. ITER—International Thermonuclear Experimental Reactor. In *Fundamentals of Magnetic Thermonuclear Reactor Design*; Woodhead Publishing Series in Energy: Sawston, UK, 2018; pp. 39–67. [CrossRef]
3. Barucca, L.; Bubelis, E.; Ciattaglia, S.; D’Alessandro, A.; Del Nevo, A.; Giannetti, F.; Hering, W.; Lorusso, P.; Martelli, E.; Moscato, I.; et al. Pre-conceptual design of EU DEMO balance of plant systems: Objectives and challenges. *Fusion Eng. Des.* **2021**, *169*, 112504. [CrossRef]
4. Available online: <https://www.euro-fusion.org/> (accessed on 10 May 2022).
5. Tarantino, M.; Martelli, D.; Del Nevo, A.; Utili, M.; Di Piazza, I.; Eboli, M.; Diamanti, D.; Tincani, A.; Miccichè, G.; Bernardi, D.; et al. Fusion technologies development at ENEA Brasimone Research Centre: Status and perspectives. *Fusion Eng. Des.* **2020**, *160*, 112008. [CrossRef]

6. Barucca, L.; Hering, W.; Martin, S.P.; Bubelis, E.; Del Nevo, A.; Di Prinzio, M.; Caramello, M.; D'Alessandro, A.; Tarallo, A.; Vallone, E.; et al. Maturation of critical technologies for the DEMO balance of plant systems. *Fusion Eng. Des.* **2022**, *179*, 113096. [[CrossRef](#)]
7. Moscato, I.; Barucca, L.; Bubelis, E.; Caruso, G.; Ciattaglia, S.; Ciurluini, C.; Del Nevo, A.; Di Maio, P.A.; Giannetti, F.; Hering, W.; et al. Tokamak cooling systems and power conversion system options. *Fusion Eng. Des.* **2022**, *178*, 113093. [[CrossRef](#)]
8. Lorusso, P.; Del Nevo, A.; Arena, P.; Eboli, M.; Marinari, R.; Tincani, A.; Agostini, P.; Badodi, N.; Cammi, A.; Del Moro, T.; et al. STEAM: A novel experimental infrastructure for the development of the DEMO BoP water coolant technology. In Proceedings of the 19th International Topical Meeting on Nuclear Reactor Thermal Hydraulics (NURETH-19), Brussels, Belgium, 6–11 March 2022.
9. Information Systems Laboratories. *RELAP5/Mod3.3 Code Manual Volume I: Code Structure, System Models, and Solution Methods*; Nuclear Safety Analysis Division, Information Systems Laboratories: Idaho Falls, ID, USA, 2001; Volume 1.
10. Ciurluini, C.; Vannoni, A.; Del Moro, T.; Lorusso, P.; Tincani, A.; Del Nevo, A.; Barucca, L.; Giannetti, F. Thermal-hydraulic assessment of Once-Through Steam Generators for EU-DEMO WCLL Breeding Blanket primary cooling system application. *Fusion Eng. Des.* **2023**, *193*, 113688. [[CrossRef](#)]
11. Available online: <https://www.babcock.com/> (accessed on 20 April 2022).
12. The Babcock & Wilcox Company. *Steam, Its Generation and Use*, 41st ed.; Kitto, J.B., Stultz, S.C., Eds.; The Babcock & Wilcox Company: Akron, OH, USA, 2005.
13. USNRC HRTD. *Pressurized Water Reactor B&W Technology, Crosstraining Course Manual, Chapter 2.4, Once-through Steam Generator*; USNRC HRTD: Washington DC, USA, 2011.
14. Ivanov, K.N.; Beam, T.M.; Baratta, A.J.; Irani, A.; Trikouros, N. *Pressurised Water Reactor Main Steam Line Break (Mslb) Benchmark*; Volume I: Final Specifications; Nuclear Energy Agency: Paris, France, 1999.
15. Spontarelli, A.M. CFD Analysis of the Aspirator Region in a B&W Enhanced Once-Through Steam Generator. Master's Thesis, Virginia Polytechnic Institute and State University, Blacksburg, VA, USA, 7 May 2013.
16. Tincani, A.; Ciurluini, C.; Del Nevo, A.; Giannetti, F.; Tarallo, A.; Tripodo, C.; Cammi, A.; Vannoni, A.; Eboli, M.; Del Moro, T.; et al. Conceptual Design of the Steam Generators for the EU DEMO WCLL Reactor. *Energies* **2023**, *16*, 2601. [[CrossRef](#)]
17. Ansys Inc. *Ansys CFX-Solver Theory Guide*; Release 2022 R1; Ansys Inc.: Canonsburg, PA, USA, 2022.
18. Water TH Properties. Available online: [http://www.peacesoftware.de/einigewerte/wasser\\_dampf\\_e.html](http://www.peacesoftware.de/einigewerte/wasser_dampf_e.html) (accessed on 8 June 2022).
19. Menter, F.R. Two-equation eddy-viscosity turbulence models for engineering applications. *AIAA J.* **1994**, *32*, 1598–1605. [[CrossRef](#)]
20. Chen, S.K.; Chen, Y.M.; Todreas, N.E. The upgraded Cheng and Todreas correlation for pressure drop in hexagonal wire-wrapped rod bundles. *Nucl. Eng. Des.* **2018**, *335*, 356–373. [[CrossRef](#)]
21. Chen, S.K.; Chen, Y.M.; Todreas, N.E. A note on the accuracy of the upgraded Cheng and Todreas correlation for predicting pressure drop in hexagonal bare rod bundles. *Appl. Therm. Eng.* **2019**, *161*, 114193. [[CrossRef](#)]

**Disclaimer/Publisher's Note:** The statements, opinions and data contained in all publications are solely those of the individual author(s) and contributor(s) and not of MDPI and/or the editor(s). MDPI and/or the editor(s) disclaim responsibility for any injury to people or property resulting from any ideas, methods, instructions or products referred to in the content.